

# Blended-Wing-Body Lateral-Directional Stability Investigation using 6DOF Simulation

Paul F. Roysdon<sup>\*</sup>

*Von Karman Institute for Fluid Dynamics, Chaussee de Waterloo 72, B-1640 Rhode-St-Genese, Belgium*

Mahmood Khalid<sup>†</sup>

*Von Karman Institute for Fluid Dynamics, Chaussee de Waterloo 72, B-1640 Rhode-St-Genese, Belgium*

Presently at the Von Karman Institute for Fluid Dynamics (VKI), a comprehensive research investigation is being performed on the lateral-directional stability characteristics of a Business Jet-class Blended-Wing-Body (BWB). This paper presents the designing attempts using lower order methods and vortex lattice based methodology to get a comprehensive understanding of the aerodynamic performance, followed by and compared with more accurate CFD methods to fine tune the performance. A multidisciplinary design and optimization code was developed and employed to tune the vehicle design with specific interest placed in the take-off and landing flight regimes where the BWB is prone stall and departure due to asymmetric wind gusts. Differential control effectors on the bottom of the wing, called "belly-flaps", are investigated for lateral-directional control. Final validation of the study is presented by applying the MDO results to aerodynamics and mass properties blocks of a six-degrees-of-freedom (6DOF) flight simulator, where landing and take-off simulations were performed with asymmetric gust loading, revealing good overall performance and stability characteristics.

## I. Relevance of the Investigation

### A. Background

Blended-Wing-Body configurations are based on the concept that the area rule provides a better aerodynamic performance from cross sectional shapes when fuselage, wings, empennage, engine pods, etc., get integrated into a single component resulting in a smooth delta shape wing body configuration. This configuration has been shown to have superior aerodynamic performance - in contrast to their classic wing-and-tube fuselage counterparts - and have reduced sensitivity to aerodynamic flutter as well as potential for increased engine noise abatement. The resulting inner space is demonstrated to cover a larger volume than the classic fuselage supported on cantilevered wings and a crossed T tail. Additionally, when the interior structure of the vehicle can be simplified with a monocoque structure, taking advantage of modern composite materials, it provides superior wing loading and structural strength. Of course without a classic tail elevator to damp the nose up pitching moment, and the vertical tail rudder to damp the yaw and possible rolling aerodynamics, the challenges in lateral roll and yaw stability, as well as pitching moment are not insignificant.

### B. Challenges and the Present Investigation

While the argument in favor of the BWB certainly is convincing, there exist significant design challenges which must be overcome. First, the lack of a horizontal and vertical tail requires that the pitch and yaw moments must be managed, at all flight conditions, by a short moment arm. Second, also related to the first, is the requirement of lateral-directional stability throughout the flight regime, most importantly at take-off

---

<sup>\*</sup>Graduate Researcher, Department of Aeronautics and Aerospace, VKI, aerodsnr@gmail.com, AIAA Member.

<sup>†</sup>Systems Engineer, Advanced Programs, Composite Engineering inc., Sacramento, California

<sup>‡</sup>Graduate Adviser, Department Chair, Department of Aeronautics and Aerospace, VKI, mahmood.khalid@nrc-cnrc.gc.ca, AIAA Senior Member.

and landing. At take-off and landing, the high angle of attack conditions make the BWB dangerously susceptible to gust loads which push the local angle of attack to near stall conditions, potentially eliminating control effectiveness of the control surfaces on the trailing edge of the wing.

The present investigation is centered around a 6 seat, business jet-class airplane, similar to the Lear 23: see figure 1. This configuration was selected because of publically available data<sup>20</sup> from which to make a comparison of the aircraft stability and performance. This paper presents the original design of a BWB configuration which exhibits favorable stability characteristics, as well as significant drag reduction and increased range performance. Particular attention will be addressed in control actuators which restore lateral-directional stability, as well as pitch stability, in the takeoff and landing flight regimes.

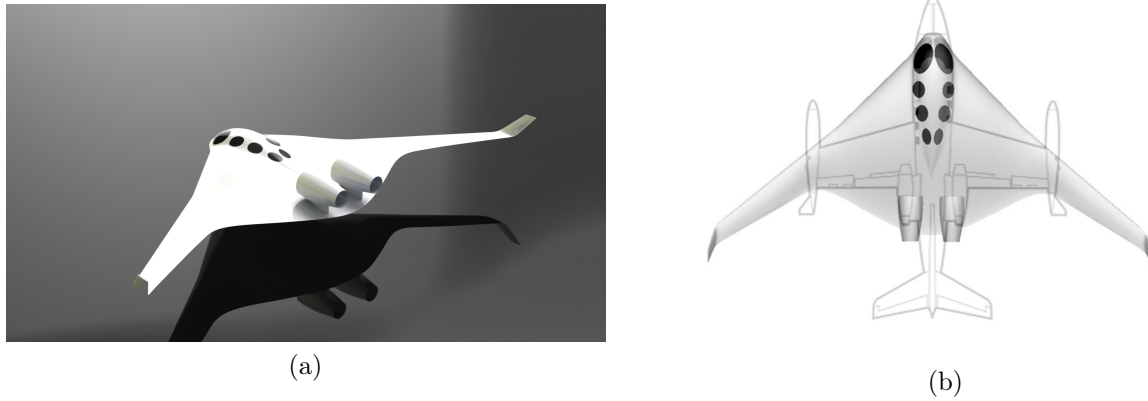


**Figure 1.** The Roysdon BWB (a), Overlay of the Roysdon BWB with a Lear 23 (b).

## II. Modeling Strategies

The initial investigation into the BWB design was first to determine a planform which was statically-stable, with aerodynamic characteristics similar to literature<sup>2,9,15,24,30</sup> and applying the literature results as a basis from which to start a multi-disciplinary design optimization, varying: inboard-to-outboard planform area, wing-sweep, wing-twist, airfoil-family, airfoil-thickness and chord length, see figure 2.

Upon obtaining a preliminary design, a study was performed on the entire angle-of-attack ( $\alpha$ ) and angle-of-side-slip ( $\beta$ ) envelope, with special interest in the lateral-directional stability characteristics. Comparing the stability coefficient results to literature data available in stability and control,<sup>1,4,6,8,16,18</sup> further investigation was performed, and an initial 6DOF simulator was developed in MatLab & Simulink. The non-linear simulation provided a benchmark from which to test the vehicle dynamics for further optimization. Later, tuning of these results would be obtained with higher-order methods, and wind tunnel analysis.

### A. Low-Order Methods

The initial investigation managed the pitch moment in two ways; first by creating pitch stability through wing sweep, and second by applying reflexed airfoils on the inboard regions of the BWB and cambered airfoil sections on the outboard regions of the BWB. The reflexed airfoil creates pitch-trim on the inboard section of the BWB, while the cambered airfoil creates two things. First, the restoring pitch-moment, common to cambered profiles, creates pitch stability. And second, the cambered profile, when combined with proper wing twist, creates the optimal lift distribution over the wing.

The pitch stability and lift distribution was obtained by applying a gradient-based optimization routine, coupling MatLab with AVL,<sup>3</sup> a vortex-lattice-method code. The MatLab-AVL optimization obtained a compromise of airfoil-family, airfoil thickness, wing sweep and wing twist, based on research findings of.<sup>9,15,24,30</sup> When the initial results were compared with those of the Boeing X-48, we find that the numerical trends are nearly identical.

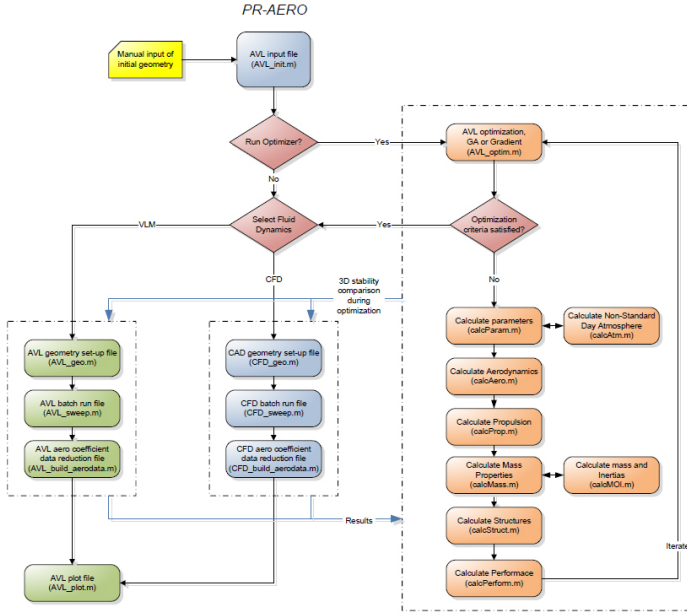


Figure 2. Coupled low-order/high-order MDO routine.

Applying the MatLab-AVL routine in a batch-mode, an analysis was performed throughout the flight envelope, with sweeps of the  $\alpha$  and  $\beta$  envelope at various velocities, resulting in an aero-database for the 6DOF simulation.

## B. High-Order Methods

A systematic approach was taken (table 1) for the investigation of the BWB using CFD, first to determine mesh dependencies on the results, and second to provide the "tuning" values needed for the first-order database:

Table 1. CFD Test Cases.

| Flight Condition | Configuration | Velocity (Mach #) | $\alpha$ (deg) | $\beta$ (deg) |
|------------------|---------------|-------------------|----------------|---------------|
| Cruise           | clean         | 0.735             | [-4,0,4,8,12]  | [0,2,6]       |
| Takeoff          | clean         | 0.183             | [-4,0,4,8,12]  | [0,2,6]       |
| Stall            | clean         | 0.098             | [4,8,12]       | [0,2,6]       |
| Takeoff          | flapped       | 0.183             | [-4,0,4,8,12]  | [-6,-2,0,2,6] |

The higher-order code in use was STAR-CCM+ v4.04, a product of CD-Adapco. Initially a half-model was tested to increase the computational speed for data acquisition and comparison to the symmetries ( $\beta=0$ ) cases of the lower-order methods (see figure 3), after which a full model was created to allow for asymmetric cases ( $\beta \neq 0$ ). Research findings show good correlation in four axes ( $F_x, F_z, M_x, M_y$ ), between the half-model CFD results and the full-model lower-order code predictions; with an average offset of less than 5%.

The initial test cases were based on a less than optimum cruise condition, Mach 0.60, because the lower-order results were obtained from an incompressible solver. Once a correlation was obtained between the lower-order method and the CFD, a full test matrix was examined. First looking at the higher Mach numbers, at the optimized cruise condition, Mach 0.73. Followed by more computationally expensive, low Mach

numbers, on the order of 0.18 Mach, representing the takeoff and landing flight regimes. In this flight regime, the BWB is prone to lateral-instabilities due to high angles-of-attack combined with asymmetric gust loads or cross-wind. The engine pods were removed on the full model to minimize number of elements in the mesh domain, and the effect on the stability is assumed to be minimal-this is considered an adequate assumption based on literature.<sup>2, 12, 15</sup>

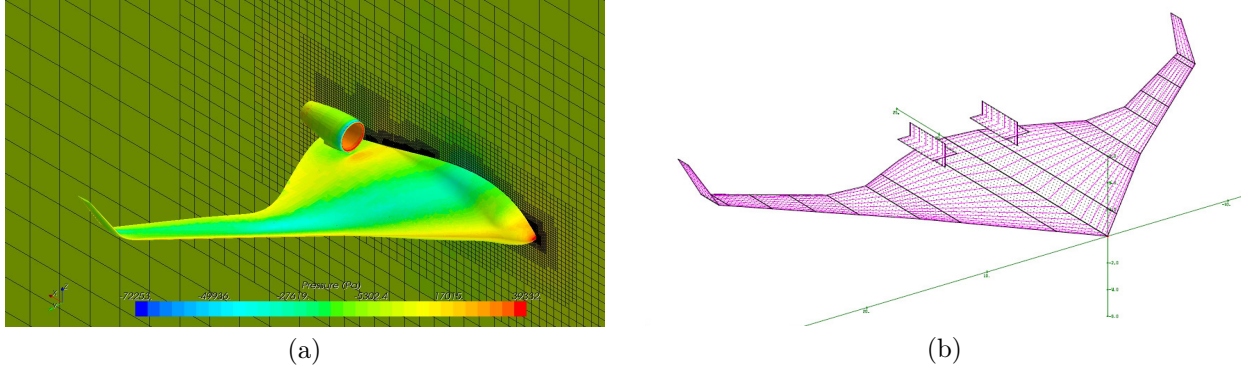


**Figure 3. BWB CFD model pressure contour (a) BWB VLM model (b).**

Following the initial investigation of  $\alpha$  and  $\beta$  sweeps, a differential control actuator was investigated based on the research by Staelens<sup>21, 22, 34</sup> investigating the pitch-moment stability created by belly-mounted flaps. While Staelens research focused on the longitudinal stability with simultaneous deployment of various belly-flap configurations, this author's investigation is in the asymmetric deployment of similar belly-flaps for lateral-directional control. This design is a common design to model-airplane enthusiasts since the late-1980's<sup>5, 23</sup> for slope-soar flying wing gliders, however no literature exists on the differential deployment of belly-flaps on the BWB configuration.

### III. Lateral-Directional Results

#### A. Aerodynamic Numerical Results

Previous design and low-order analysis attempts into the lateral-directional stability revealed that the BWB was more stable with the belly-flaps deployed. This result was anticipated, however higher-order methods revealed a strong roll-yaw coupling induced by the belly-flaps. Both single and combined/differential belly-flap configurations were evaluated with flap deployments at 30, 60, and 90 degrees perpendicular to the flow. It was found that single, right-side or left-side only, deployment of the flaps at 60-90 degrees increased the yaw stability dramatically while simultaneously decreasing the roll stability. Further analysis revealed that full flap deployment of one side (i.e. right-hand-side) and partial flap deployment of the opposite side (i.e. left-hand-side) maintained the pitch stability – a similar configuration to Staelen's research – while also providing greatly improved roll and yaw stability. These results have been compiled into surface plots and compared to the lateral-directional stability of a Lear 23, see figures 4, 5, and 6. The findings reveal that the present BWB configuration demonstrates stronger lateral-directional stability (solid-mesh) over the Lear 23 (open-mesh), with the final figure depicting the streamlines over the BWB with the right-hand flap deployed at 60 degrees, at an angle-of-attack of zero degrees and angle-of-side-slip of 12 degrees.

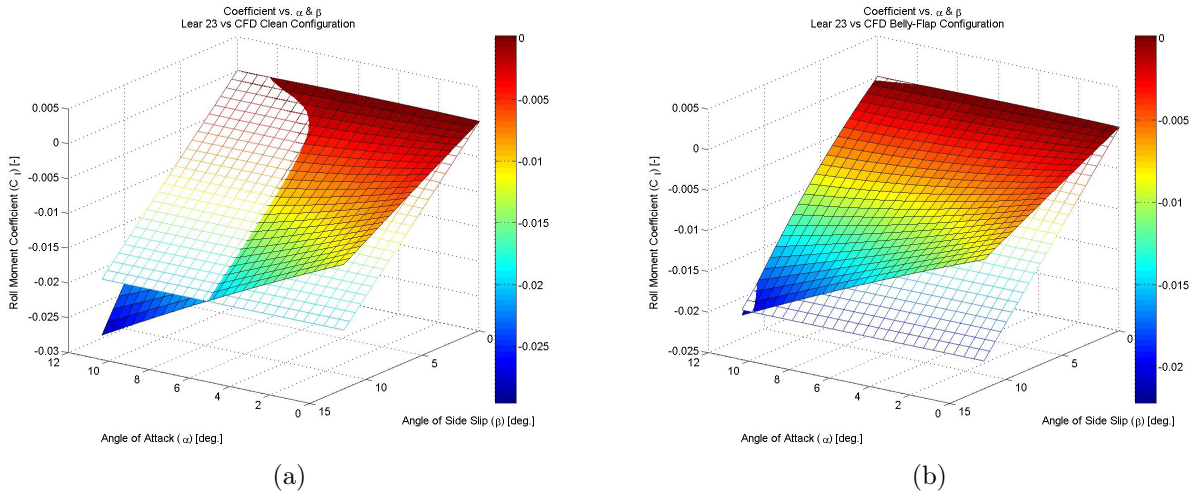


**Figure 4. BWB vs. Lear 23 Roll Moment comparison - BWB no flap (a) BWB belly-flap deployed (b).**

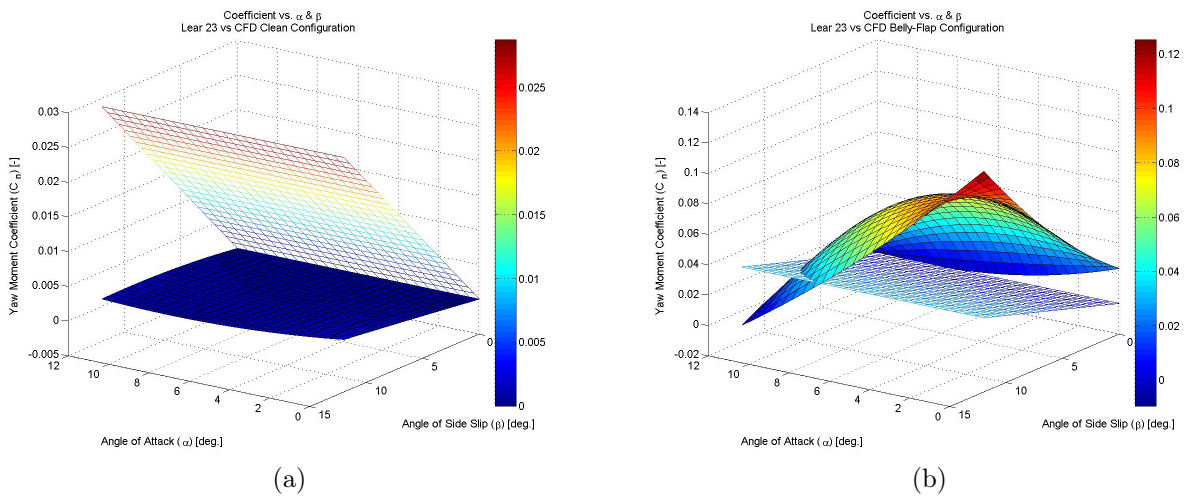


**Figure 5. BWB vs. Lear 23 Yaw Moment comparison - BWB no flap (a) BWB belly-flap deployed (b).**

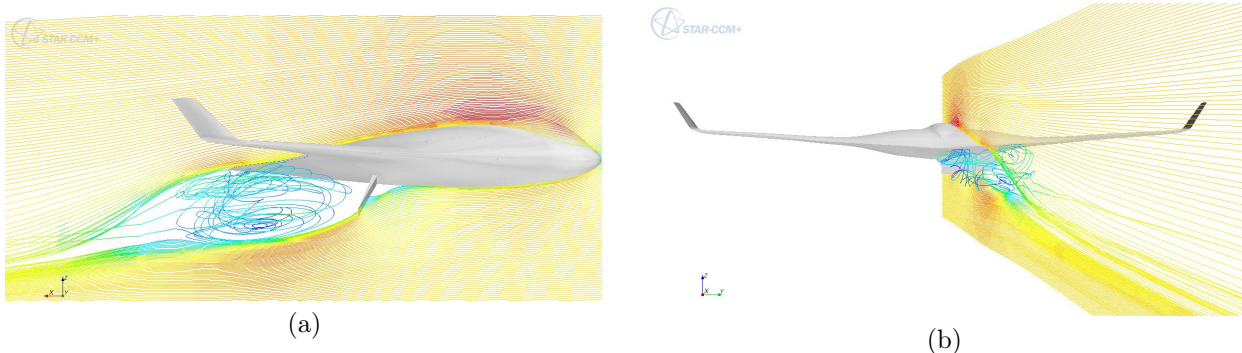


**Figure 6. R.H. Belly Flap CFD streamline profiles [velocity magnitude] for  $\alpha=0^\circ$ ,  $\beta=12^\circ$  - side (a) aft (b).**

## B. Flight Simulation Results

A flight simulation was performed using a complete 6DOF flight simulator created in MatLab & Simulink. The flight simulator was developed with the MDO routine in-mind such that the aerodynamics, mass properties, engine and sensor models could be quickly generated and adapted to a new design. The simulator uses a *relatively* simple autopilot for guidance and control. A complete Integrated Navigation System (INS) was used, that employs a simulated GPS receiver, an inertial measurement unit (IMU) and a pitot-static system, as well as a 34-state tightly-coupled Navigation Kalman Filter (NKF) and Strap-down Navigator (SDN). Additionally, the simulator uses a complete suite of environmental models: wind, gust and turbulence models, a non-standard day atmospheric model and a WGS-84 earth geode model. The structure of the simulation is comprised of both Simulink blocks and Embedded MatLab code, capable of C-code generation for hardware in the loop (HWIL) for testing of the navigation and guidance loops.

### 1. High-Altitude Testing

Initial flight scenarios were performed at altitude to test the system as a unit. Pitch and Roll commands were performed in both open-loop and closed-loop test scenarios, evaluating basic stability and control surface effectiveness, and allow for autopilot gain tuning. In figures 7 - 10, a standard rate turn was commanded, demonstrating very favorable stability with more than adequate control surface effectiveness. These results are of course also a function of control gain within the autopilot; however, the system shows promise for good control at lower altitude and slower speeds where the vehicle is prone to stall and departure from controlled flight.

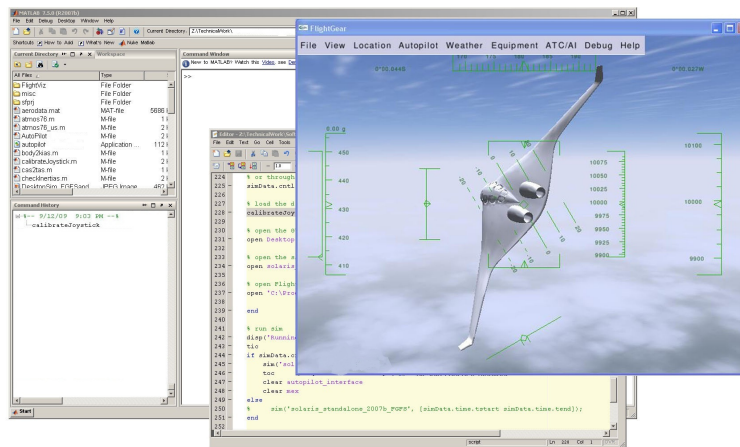


**Figure 7. Flight Simulation: BWB 60 degree roll. Visual aid using Flight Gear Flight Sim.**

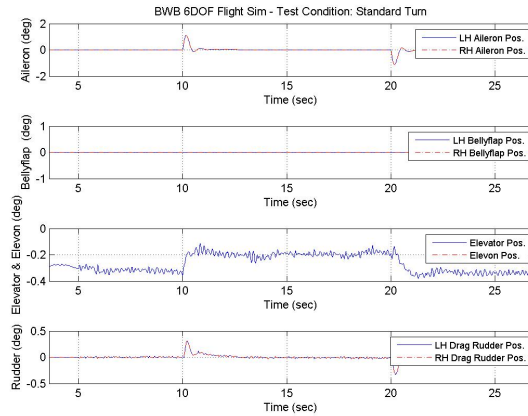


**Figure 8. Flight Simulation: Control Surface results.**

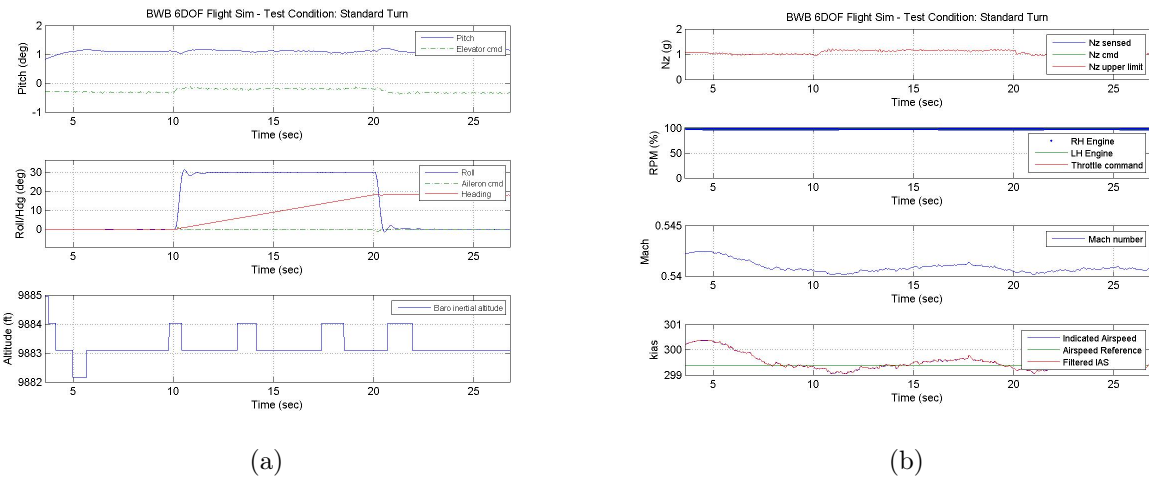


**Figure 9. Flight Simulation: Euler Angles and Altitude (a) Acceleration, Engine RPM% and Velocity (b).**

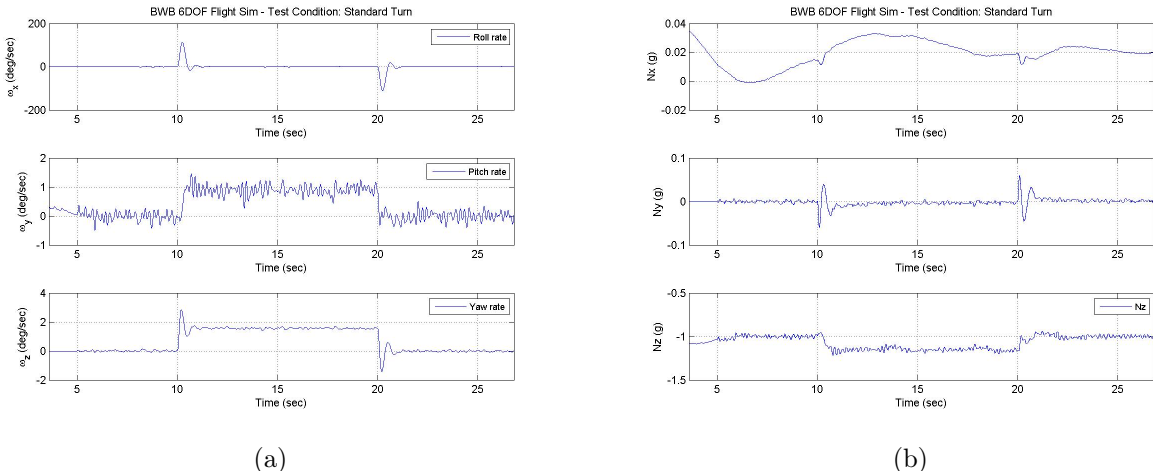


**Figure 10. Flight Simulation: Angular Rates (a) Linear Accelerations (b).**

## 2. Landing and Takeoff Testing

The initial high-altitude simulations provided the information necessary to integrate the belly-flap control strategy. Complete landing and take-off simulation where then performed, with simulated calm to violent wind and gust test conditions. A Monte Carlo Analysis (MCA) approach was employed with over 10,000 test cases demonstrated. The Denver International Airport was used as a point of reference to evaluate the BWB under the most harsh conditions that would likely be seen in the United States FAA airspace, with extreme heat and wind at high altitude.

### Simulated Takeoff and Landing Location

- Airport: Denver International (KDEN), Denver, Colorado, United States
- Location:  $39.86^{\circ}$  N,  $104.67^{\circ}$  W
- Field Elevation: 5,431 feet MSL
- Light-Aircraft Pattern Altitude: 6,431 feet MSL
- Runway: 16L

Historical data was obtained<sup>31</sup> and evaluated for maximum, minimum and average conditions for temperature, pressure, wind and wind-direction during each of the four annual seasons. This historical weather data was applied to the MCA bounds for a normal distribution of randomized atmospheric conditions as shown in table 2. Initial flight conditions were set-up for landing and takeoff on runway 16L – a heading of 160 degrees – at Denver, with a landing entry from pattern altitude of roughly 1000 feet AGL.

**Table 2. MCA Weather Conditions.**

| Condition      | Units        | Min. | Max.  |
|----------------|--------------|------|-------|
| Wind Speed     | knots        | 0.0  | 40    |
| Wind Direction | deg          | 0.0  | 359.9 |
| Gust Speed     | knots        | 0.0  | 55    |
| Gust Direction | deg          | 0.0  | 359.9 |
| Temperature    | $^{\circ}$ F | 15.0 | 105.0 |
| Altimeter      | deg          | 29.1 | 30.6  |

Failure of each MCA case was based on the conditions set fourth in table 3. The *Primary Factors* established safe flying conditions for the vehicle within airport airspace based on extreme weather conditions and vehicle limitations. The *Secondary Factors* are less strict due to the lack of auto-land functionality within the autopilot algorithms of the flight simulator. To add this additional functionality, a control loop would be required, using GPS Latitude/Longitude along with a Radar Altimeter for precise positional information. Furthermore, to properly setup each case, a "straight-in" arrival would need to be assumed such that the Ordinary Differential Equation (ODE) solver within the 6DOF simulator, could reach a steady state prior to data collection. This requires the simulator to account for vehicle kinematics and atmospheric conditions, and to allow the auto-land control loop of the autopilot to assess the wind condition such that a landing trajectory could be calculated, and similarly for the takeoff trajectory. To do this adds both additional simulation time and complexity that could be easily solved with further analysis of the MCA results. Therefore simplicity and faster simulation time was chosen, and the results were assessed similar to the following example.

Consider a particular MCA landing simulation where the vehicle remained safely within the *Primary Factors* but landed below the field elevation; if the *Altitude* was considered a strict violation of the MCA Failure Criteria, the simulation would have been a failure. However, in the simplified simulator approach,

this simulation remained within safe vehicle operational bounds and therefore considered a success of vehicle control at landing conditions. Again the primary goal is to assess the lateral-directional stability of the vehicle at landing and takeoff conditions – i.e. high  $\alpha$ , high  $\beta$ , and low velocity – where the vehicle is prone to asymmetric stall and departure.

**Table 3. MCA Failure Criteria.**

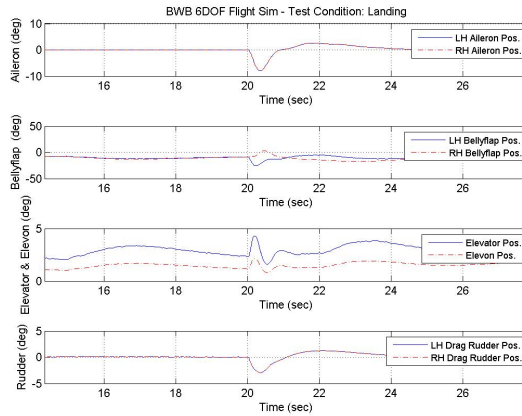
| Primary Factors                |       |          |          |
|--------------------------------|-------|----------|----------|
| Condition                      | Units | Landing  | Takeoff  |
| Roll                           | deg   | $\pm 30$ | $\pm 40$ |
| Pitch                          | deg   | -10/+30  | 0/+40    |
| angle-of-attach ( $\alpha$ )   | deg   | -6/+16   | -6/+16   |
| angle-of-side-slip ( $\beta$ ) | deg   | $\pm 12$ | $\pm 12$ |

| Secondary Factors |       |          |          |
|-------------------|-------|----------|----------|
| Condition         | Units | Landing  | Takeoff  |
| Altitude          | deg   | $\pm 50$ | $\pm 50$ |
| Heading           | deg   | $\pm 10$ | $\pm 50$ |

Of the 10,000 simulations, less than 8% of the landing cases failed and less than 5% of the takeoff cases failed. The primary difference between the two scenarios is the energy state of the vehicle. Upon landing, the vehicle is more prone to stall and exhibits the common characteristics of a "Power-OFF stall." While in the takeoff scenario, characteristics of a "Power-ON stall" were seen, however the greater thrust-to-drag ratio at takeoff nearly overcomes the stall onset in most cases. Additionally, the strict takeoff failure criteria was reduced simply because the vehicle is not limited to a landing strip, and was therefore allowed to veer off course heading – though in reality this would most likely violate air-traffic safety.

The following figures depict the successful landing and takeoff trajectories as a function of time; first for a single simulation scenario (figures 11 - 13) and then for the MCA results (figures 14 - 17), followed by histograms of the 10k test cases (figures 18 - 21), and polar plots of the wind magnitude and direction of the failed cases (figures 22 & 23). In figures 11 - 13, the simulation was initialized without wind, followed by activating the wind at 5 seconds, followed by the gust at 20 seconds – just after the flare when the vehicle is most prone to stall. Because of simulation initial conditions, oscillations in the data exist during the first few seconds as the simulator ODE solver converges on a solution. In the landing trajectories, the "flare" prior to touchdown, was commanded at 15 seconds and the vehicle was considered to be in ground-effect thereafter. The landing assumed a worst case of an engine-out emergency landing, which imposes a glide at the best L/D. An engine-out landing forces the vehicle to be controlled strictly using the control surfaces, and no residual thrust or windmill drag was applied to the simulation. In the takeoff trajectories, a short runway takeoff was simulated, and a pitch of 5 degrees was commanded until the airspeed was sufficiently high, upon which a 15 degree climbout was commanded. In all cases, roll was commanded to hold 0 degrees and course heading was commanded to hold 160 degrees – runway heading. For all MCA cases, the wind module remained on during the entire simulation, and gusts were started randomly between 5-25 seconds. This is most easily recognized in the Roll attitude plots, figures 14(b) & 16(b). For readability the  $\beta$  figures, 15(b) & 17(b), were only plotted for wind/gust on one side of the vehicle. This allows the reader to see the yaw excursion with an immediate return to a nominal attitude. Notice also the strong roll-yaw coupling; this is characteristic of this vehicle, and in particular a partial result of the belly-flap control.



**Figure 11. Successful Landing: Control Surface results.**

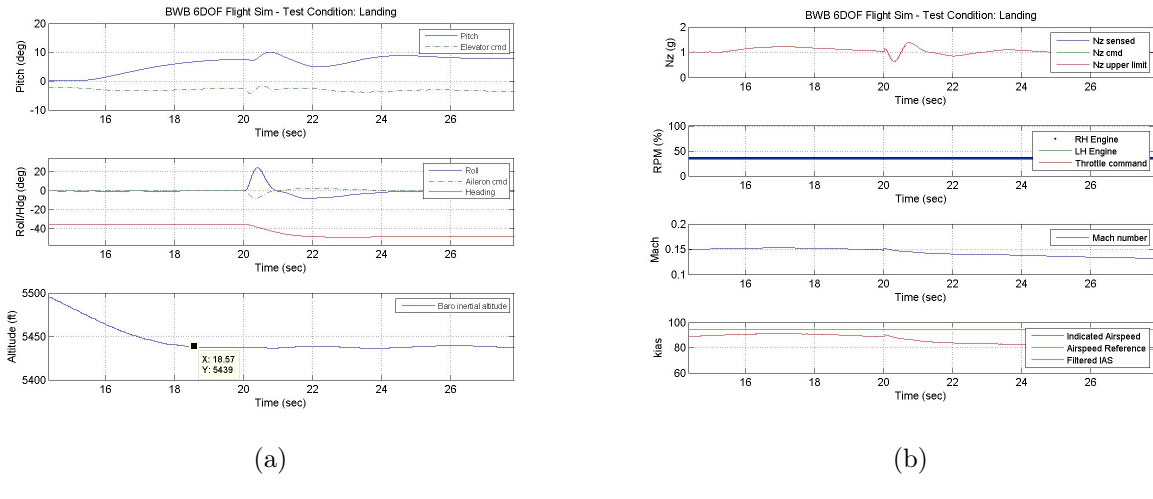


**Figure 12. Successful Landing: Euler Angles and Altitude (a) Acceleration, Engine RPM% and Velocity (b).**

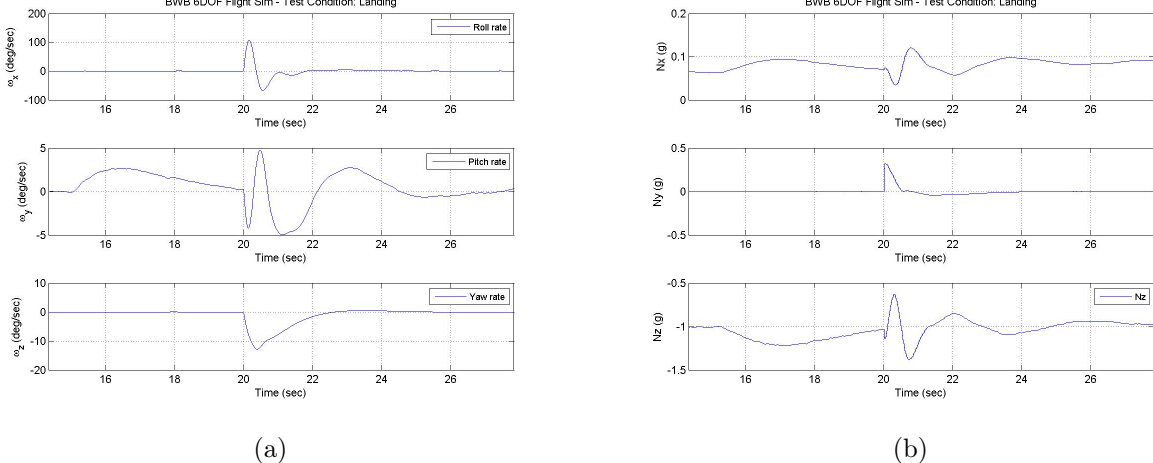


**Figure 13. Successful Landing: Angular Rates (a) Linear Accelerations (b).**

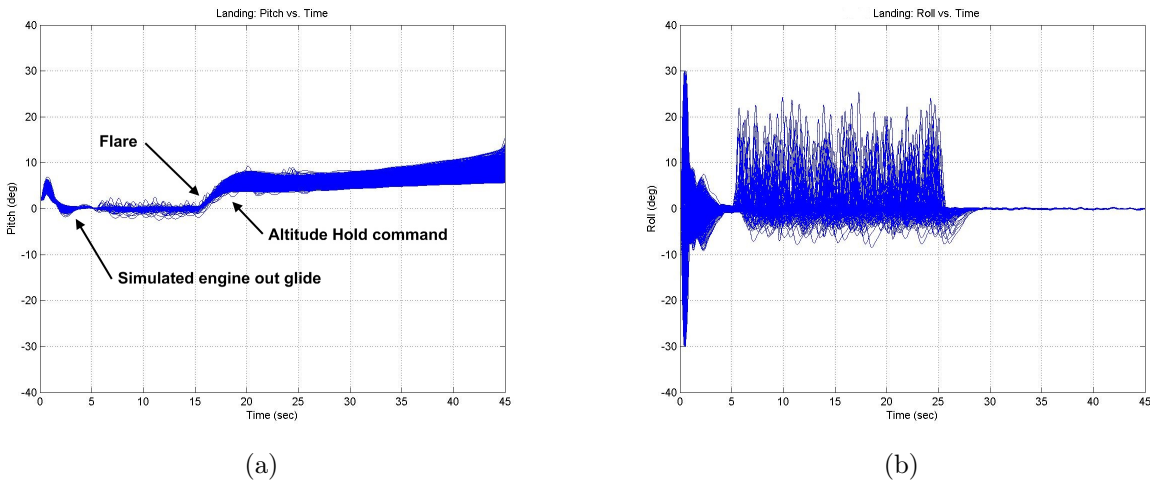


**Figure 14. Landing: Pitch (a) Roll (b).**

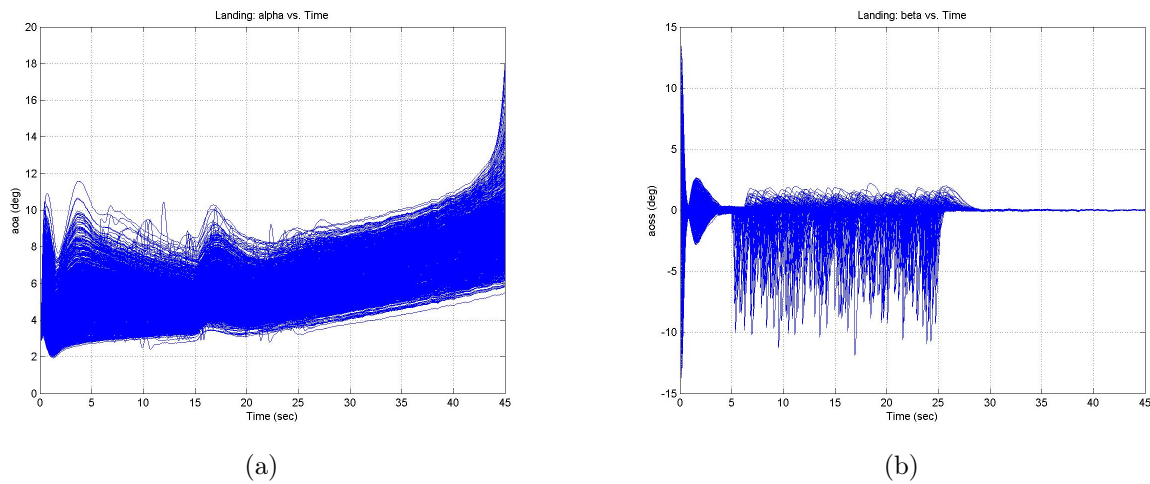


**Figure 15. Landing:  $\alpha$  (a)  $\beta$  (b).**

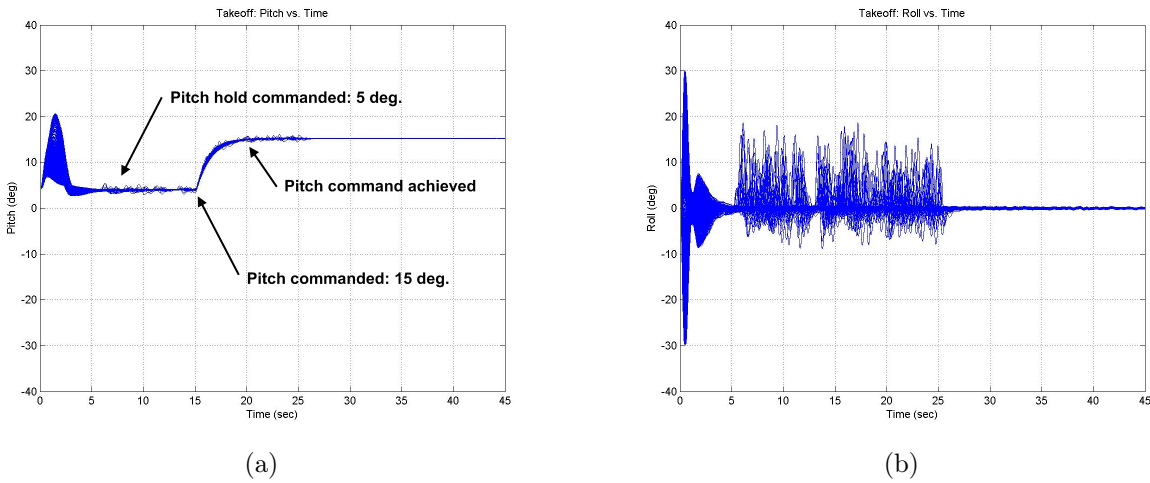


**Figure 16. Takeoff: Pitch (a) Roll (b).**

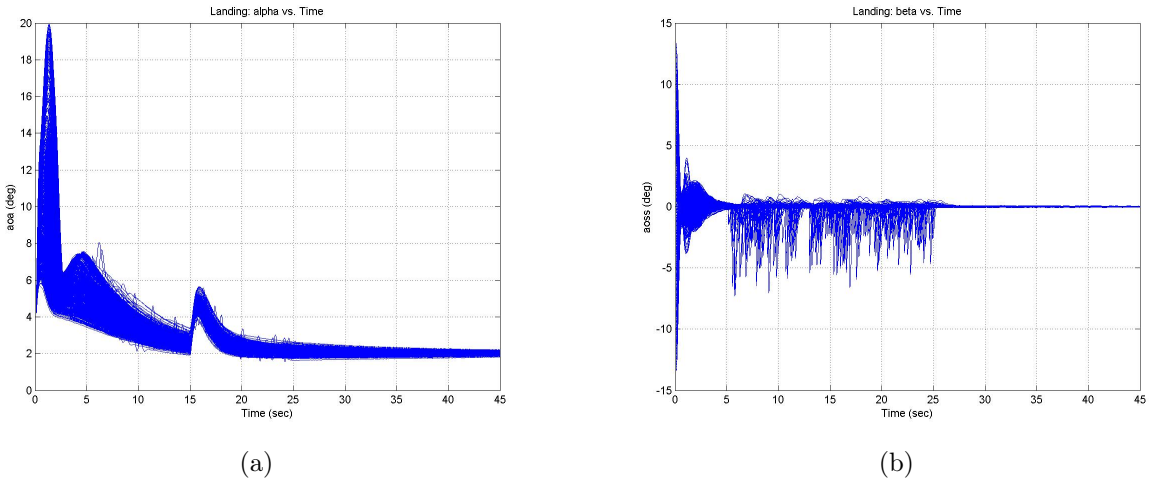


**Figure 17.** Takeoff:  $\alpha$  (a)  $\beta$  (b).

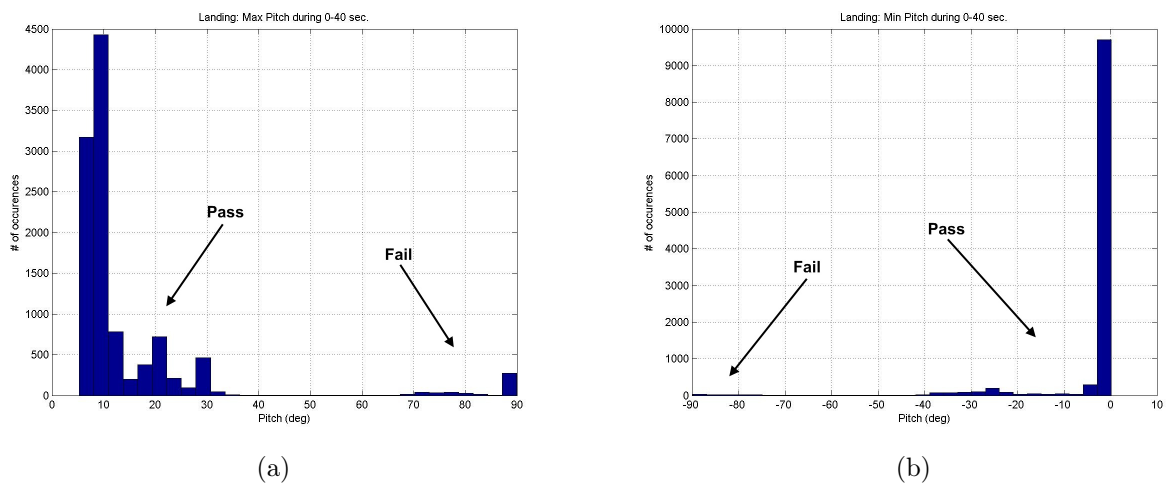


**Figure 18.** Landing Pitch angle: Min. (a) Max. (b).

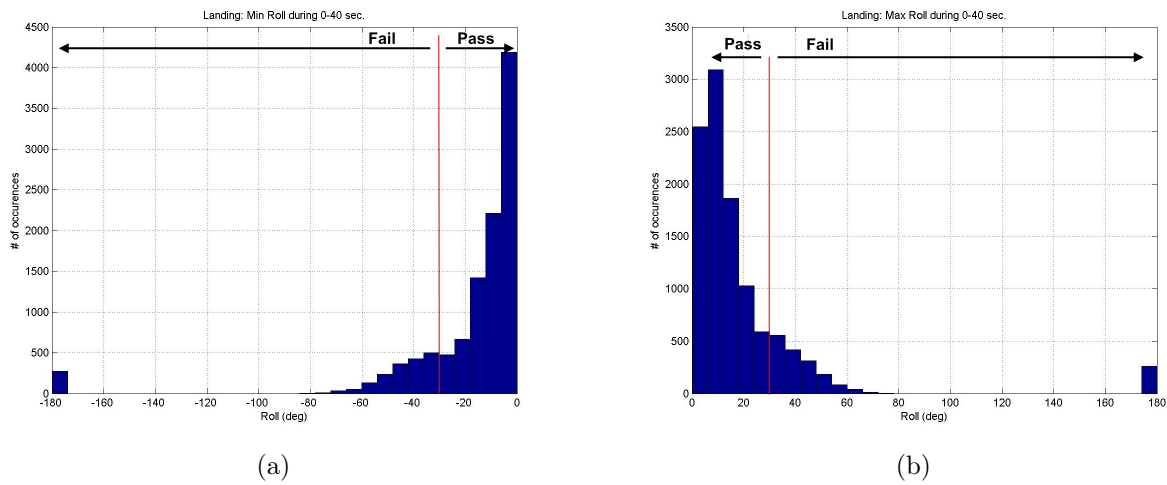


**Figure 19.** Landing Roll angle: Min. (a) Max. (b).

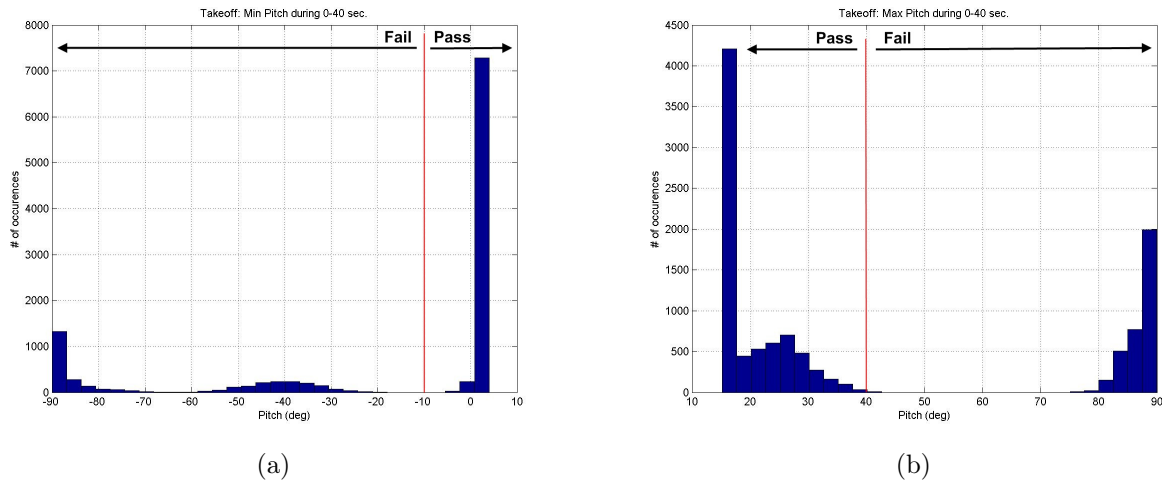


**Figure 20. Takeoff Pitch angle: Min. (a) Max. (b).**

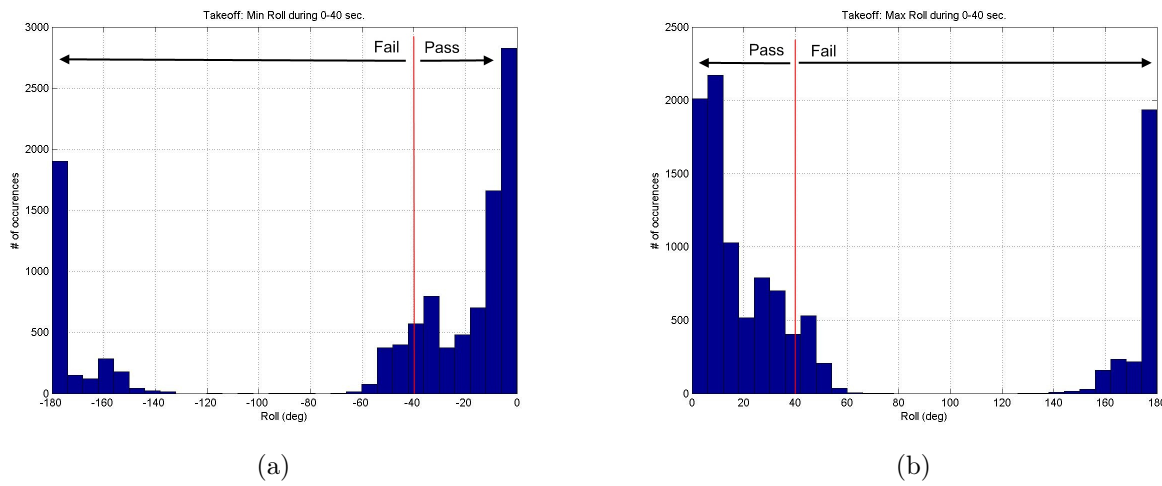


**Figure 21. Takeoff Roll angle: Min. (a) Max. (b).**

Considering figures 22 & 23 it is interesting to note that the temperature, and consequently the density altitude (altimeter), was not a driving factor in the failed test conditions. The polar plots show a near even distribution of temperature variation to wind speed and direction. This demonstrates that the BWB stability is driven primarily by the wind condition. Amazingly, the BWB demonstrates a similar maximum crosswind component limitation to the Lear, of 24 knots magnitude at 90 (270) degrees to the course heading. While the BWB is certainly more sensitive to crosswind than the Lear, the BWB is however performing at or near other aircraft of its class, and well above small aircraft like a Cessna-172N which has a maximum crosswind component of 15 knots.

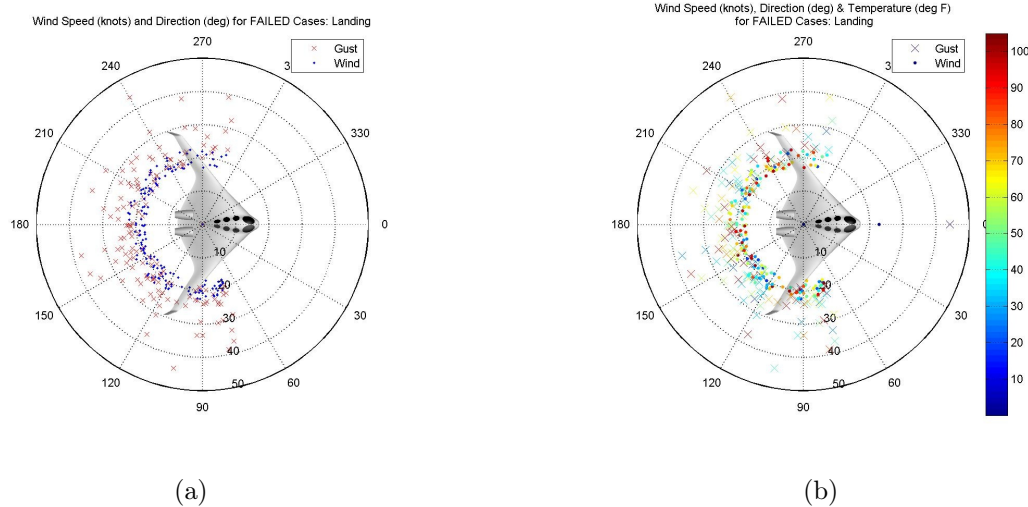


**Figure 22. Landing: Failed cases for wind & gust magnitude and direction (a) with temperature (b).**

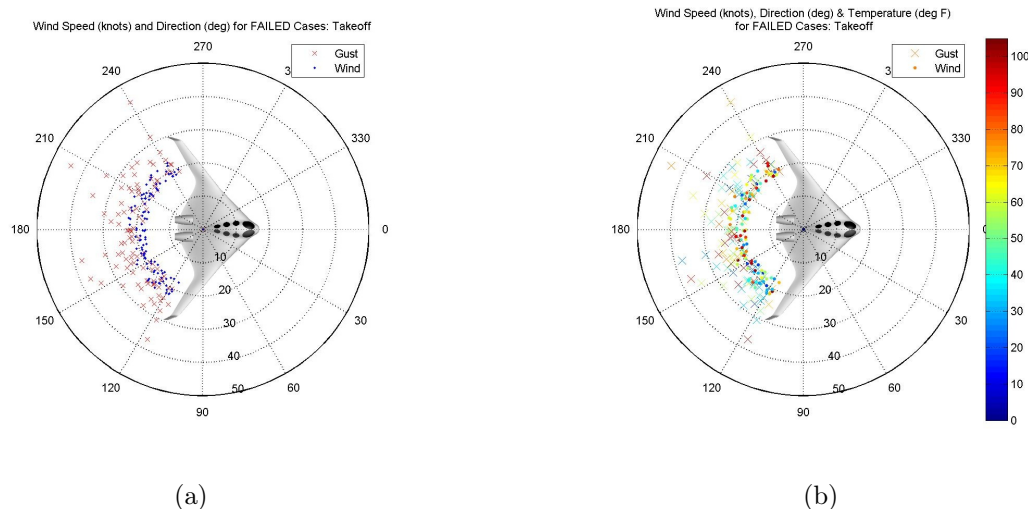


**Figure 23. Takeoff: Failed cases for wind & gust magnitude and direction (a) with temperature (b).**

## IV. Concluding Remarks

The present investigation into the lateral-directional stability of the BWB configuration, reveals that higher-order methods confirm the findings, with increased accuracy, compared with the lower-order methods. Initial results reveal that the present configuration is statically stable, however with 25-40% reduced stability when compared with the Lear 23 coefficients<sup>11,13,20</sup>. Initial belly-flap analysis improves this stability delta to a range of 10-15% or better. This investigation has also shown design success through extensive 6DOF flight simulation testing, using a high fidelity MatLab-Simulink model for takeoff, landing and go-around trajectories. High-order analysis is continuing to validate the use of bell-flap control surfaces for lateral-directional control, and both wind-tunnel test and flight test data of a dynamically scaled flight demonstrator will provide additional confidence in the present investigation findings.

## V. Acknowledgments

I would like to thank my Von Karman Institute research advisor Mahmood Khalid, for his guidance and technical reviews of this research. I would also like to thank the faculty and staff at the Von Karman Institute for making this research a possibility and a reality. I could not have achieved so much in so little time without their academic facilities, thought provoking coursework and applied research. Finally, I would like to thank Mike and Amy Fournier - the owners at Composite Engineering inc. - as well as Doug Meyer and Dan Raymer - my industry mentors - without these people I would not have the phenomenal aircraft design, analysis, and flight test experience with several high performance jet aircraft. Thank you all.

## References

- <sup>1</sup>Buffington, J.M., "Tailless Aircraft Control Allocation", AIAA-97-3605.
- <sup>2</sup>Carter, M.B., *et.al.*, "Blended-Wing-Body Transonic Aerodynamics: Summary of Ground Tests and Sample Results (Invited)", A47th AIAA Aerospace Sciences Meeting Including the New Horizons Forum and Aerospace Exposition, 5-8 January 2009, Orlando, Florida. AIAA-2009-935.
- <sup>3</sup>Drela, M., Youngren, H., AVL 3.26 User Primer. MIT Aero & Astro. 29 Apr 2006. <<http://web.mit.edu/drela>>.
- <sup>4</sup>Iniguez de Heredia, A., Frichmelt, H., "GN&C Concepts for a Blended Wing Body", AIAA Guidance, Navigation, and Control Conference, 15-18 August 2005, San Francisco, California. AIAA-2005-6351.
- <sup>5</sup>Kuhlman, B., Kuhlman, B., "On the 'Wing... the book", vol. 1-4, *B<sup>2</sup>Streamlines*, Washington, 1993-2004.
- <sup>6</sup>Leman, T., *et.al.*, " $\lambda_1$  Adaptive Control Augmentation System for the X-48B Aircraft", AIAA Guidance, Navigation, and Control Conference, 10-13 August 2009, Chicago, Illinois. AIAA-2009-5619.
- <sup>7</sup>Liebeck, R.H., "Design of the Blended Wing Body Subsonic Transport", American Institute of Aeronautics & Astronautics Journal of Aircraft, Vol. 41, No. 1, January-February 2004. AIAA-9084-368.
- <sup>8</sup>McKeehen, P.D., "Genesis Non-Realtime Simulation of a Tailless Aircraft", AIAA-98-4159.
- <sup>9</sup>Mialon, B., Fol, T., Bonnaud, C., "Aerodynamic Optimisation of Subsonic Flying Wing Configurations", 20th AIAA Applied Aerodynamics Conference, 24-26 June 2002, St. Louis, Missouri. AIAA-2002-2931.
- <sup>10</sup>Morris, A.M., Allen, C.B., Rendall, T.C.S., "Aerodynamic Optimisation of Modern Transport Wing using Efficient Variable Fidelity Shape Parameterization", 47th AIAA Aerospace Sciences Meeting Including the New Horizons Forum and Aerospace Exposition, 5-8 January 2009, Orlando, Florida. AIAA-2009-1277.
- <sup>11</sup>Nelson, R., *Flight Stability and Automatic Control*, McGraw-Hill, 2nd ed., 1997.
- <sup>12</sup>Peigin, S., *et.al.*, "Computational Fluid Dynamics Driven Optimisation of a Blended-Wing-Body Aircraft", AIAA Journal, Vol. 44, No. 11, November 2006. AIAA-19757-954.
- <sup>13</sup>Roskam, J., Lan, C.E., *Airplane Flight Dynamics and Automatic Flight Controls*, Darcorporation, Vol.1-2, 2003.
- <sup>14</sup>Qin, N., *et.al.*, "Spanwise Lift Distribution for a Blended Wing Body Aircraft", AIAA Journal of Aircraft, Vol. 42, No.

2, March-April 2005. AIAA-4229-140.

<sup>15</sup>Qin, N., "Aerodynamic Studies for Blended Wing Body Aircraft", 9th AIAA/ISSMO Symposium on Multidisciplinary Analysis and Optimisation, 4-6 September 2002, Atlanta, Georgia. AIAA-2002-5448.

<sup>16</sup>Regan, C.D., "In-Flight Stability Analysis of the X-48B Aircraft", AIAA Atmospheric Flight Mechanics Conference and Exhibit, 18-21 August 2008, Honolulu, Hawaii. AIAA-2008-6571.

<sup>17</sup>Risch, T., *et.al.*, "X-48 Flight-Test Progress Overview", A47th AIAA Aerospace Sciences Meeting Including the New Horizons Forum and Aerospace Exposition, 5-8 January 2009, Orlando, Florida. AIAA-2009-934.

<sup>18</sup>Stephan, S., van Dam, C.P., "Determination of Wing-Only Aircraft Tumbling Characteristics Through Computational Fluid Dynamics", AIAA Journal of Aircraft, Vol. 45, No. 3, May-June 2008. AIAA-33730-763.

<sup>19</sup>Schrenk, O., "A simple approximation method for obtaining the spanwise lift distribution", National Advisory Committee for Aeronautics, April 1940, naca-tm-948.

<sup>20</sup>Soderman, P., Aiken, T., "Full-Scale Wind-Tunnel Tests of a Small Unpowered Jet Aircraft With a T-Tail", NASA Ames Research Center, November 1971), NASA TN D-6573.

<sup>21</sup>Staelens, Y. D., Blackwelder, R. F., and Page, M. A., "Novel Pitch Control Effectors for a Blended-Wing-Body Airplane in Takeoff and Landing Configuration", AIAA Paper 2007-68-229, January 2007.

<sup>22</sup>Staelens, Y. D., Blackwelder, R. F., and Page, M. A., "Study of Belly-flaps to Enhance the Lift and Pitching Moment Coefficient of a Blended-Wing-Body Airplane , AIAA Paper 2007-4176, June 2007.

<sup>23</sup>Stokely, H.A., *et.al.*, "Soar-Tech", vol. 1-10, Herk Stokely (Editor), SoarTech Journal, Virginia, 1982-1993.

<sup>24</sup>Valiyff, A., Arjomandi, M., "An Investigation into the Aerodynamic Efficiency of a Tailless Aircraft", 47th AIAA Aerospace Sciences Meeting Including the New Horizons Forum and Aerospace Exposition, 5-8 January 2009, Orlando, Florida. AIAA-2009-1436.

<sup>25</sup>Vicroy, D.D., "Blended-Wing-Body Low-Speed Flight Dynamics: Summary of Ground Tests and Sample Results (invited)", 47th AIAA Aerospace Sciences Meeting Including the New Horizons Forum and Aerospace Exposition, 5-8 January 2009, Orlando, Florida. AIAA-2009-933.

<sup>26</sup>Wakayama, S., Kroo, I., "The Challenge and Promise of the Blended-Wing-Body Optimisation", AIAA Paper 98-4736, in Proceedings of 7th AIAA Symposium on Multidisciplinary Analysis and Optimization, St Louis, MO, September 1998, pp. 239-250.

<sup>27</sup>Wakayama, S., Willcox, K., "Simultaneous Optimisation of a Multiple-Aircraft Family", AIAA.

<sup>28</sup>Wakayama, S., Kroo, I., "Subsonic Wing Planform Design Using Multidisciplinary Optimization", Journal of Aircraft, Vol. 32, No. 4, Jul.-Aug. 1995, pp.746-753.

<sup>29</sup>Wakayama, S., Page, M., Liebeck, R., "Multidisciplinary Optimization on an Advanced Composite Wing", AIAA Paper 96-4003 presented at 6th AIAA Symposium on Multidisciplinary Analysis and Optimization, Bellevue, WA, September 4-6, 1996.

<sup>30</sup>Wakayama, S., "Multidisciplinary Optimization of the Blended-Wing-Body", AIAA Paper 98-4938, in Proceedings of 7th AIAA Symposium on Multidisciplinary Analysis and Optimization, St Louis, MO, September 1998, pp. 1771-1779.

<sup>31</sup>Weather Underground, <<http://www.weatherunderground.com>>

<sup>32</sup>Whitcomb, R.T., "A Study of the Zero-Lift Drag-Rise Characteristics of Wing-Body Combinations Near the Speed of Sound", National Advisory Committee for Aeronautics, 1952. NACA-RM-L52H08.

<sup>33</sup>Wood, R.M., Bauer, S.X.S., "Flying Wings/Flying Fuselages", 39th AIAA Aerospace Sciences Meeting & Exhibit, Reno, Nevada, 8-11 January 2001. AIAA-2001-0311.

<sup>34</sup>Yann, D.S., *et.al.*, "Computer Simulation of Landing, Takeoff and Go-around of a Blended-Wing-Body Airplane with Belly-Flaps", AIAA Conference, 7-10 January 2008, Reno, Nevada. AIAA-2008-297.